



A wide aperture telescope for high energy gamma rays detection

G. Barbiellini^a, M. Boezio^a, M. Candusso^b, M. Casolino^b, M. P. De Pascale^b, C. Fuglesang^c, A. M. Galper^d, A. Moiseev^d, A. Morselli^{b*}, Yu. V. Ozerov^d, P. Picozza^b, A. V. Popov^d, M. Ricci^e, R. Sparvoli^b, P. Spillantini^f, A. Vacchi^a, S.A. Voronov^d, V. M. Zemskov^d, V. G. Zverev^d

^a Dept. of Physics, Univ. of Trieste and INFN, Italy

^b Dept. of Physics, Univ. of Rome "Tor Vergata" and INFN, Italy

^c Royal Institute of Technology, Stockholm, Sweden

^d Moscow Engineering Physics Institute, Moscow, Russia

^e INFN Laboratori Nazionali di Frascati, Italy

^f Dept. of Physics, Univ. of Firenze and INFN, Italy

In this paper new techniques for the realization of a high energy gamma-ray telescope are presented, based on the adoption of silicon strip detectors and lead scintillating fibers. The simulated performances of this instrument show that the silicon strip technology adopted by GILDA (Gamma-ray Imaging Large Detector for Astrophysics) could improve the performance of EGRET, which is so far the most successful experiment of a high energy gamma-ray telescope, though having less volume and weight.

1. Introduction

High energy gamma-ray astrophysics has greatly developed in these last few years because of the results of the experiment EGRET[1] on the Compton Gamma Ray Observatory. The satellite observations have brought more detailed data about the well known gamma-ray sources, but also the discovery of new ones, both galactic and extragalactic, especially Active Galactic Nuclei and gamma-ray bursts. All these exciting results have shown the necessity of a next generation experiment with a sensitivity increased by at least one order of magnitude and with better angular and energetic resolutions.

We will show in this paper that tracking systems based on silicon strip technology can be the solution to the above demands. Besides, they have the advantage of not requiring high voltages or photomultipliers (low consumption), offer the possibility of self-triggering, avoid the use of consumable materials (gas) and allow a drastic dead time reduction.

2. The GILDA apparatus

The core of the GILDA telescope is a modified space version of the silicon calorimeter presently used in the Wizard balloon flights program [2], to be installed on a future version of the Russian Resource-01 satellite.

The calorimeter performance has been studied with Monte Carlo simulations[3]. A prototype, containing 20 XY samplings of 6×6 cm² silicon wafers with strips 3.6 mm wide [4] interleaved with showering tungsten planes, has already been tested at the CERN Proton Synchrotron (PS) [5]. Connecting together this wafers, planes of different area can be formed. A 50×50 cm² has already flown in balloon-borne experiments from NASA bases of Fort Sumner (New Mexico), in September 1993 (5 planes), and Lynn Lake (Canada), in August 1994 (8 planes).

The main constraints for the telescope are imposed by the satellite in terms of volume, weight and available electric power. The free volume on the satellite is a cylinder 110 cm in diameter and 70 cm in height, the available mass

*Corresponding author

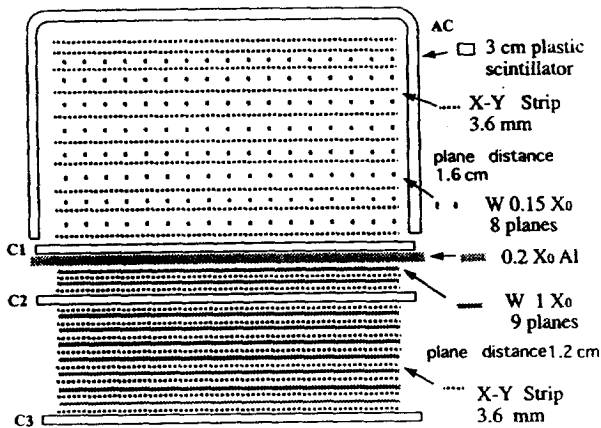


Figure 1. The stratigraphy of the GILDA A detector (not to scale).

and electric power are, respectively, 400 kg and 350 W.

2.1. Configuration A

We have considered the use of the same silicon calorimeter of the balloon flights, 11.5 radiation lengths (X_0) thick, for a total height of 40 cm, 50×50 cm² wide in area and 64 degrees of aperture.

The stratigraphy of the calorimeter is shown in fig. 1. The structure can be separated into two sections: the converter and the absorber. The first ten planes form the converter zone, where the silicon planes, except the top two, are separated by tungsten plates of $0.15 X_0$ thickness. The last ten planes, separated by tungsten plates of $1 X_0$ thickness, except for the first that has aluminum ($0.2 X_0$) in place of tungsten, form the absorber. The aluminum plate is placed in order to reduce the back scattering of particles.

The converter is covered with a system of anticoincidence scintillator counters. Three plastic scintillation counters (C1, C2, C3) with a characteristic time of the order of 20 ns, have been included in the apparatus for the trigger.

The first level trigger (fast) is then formed by the coincident pulses from C1, C2, C3 and the

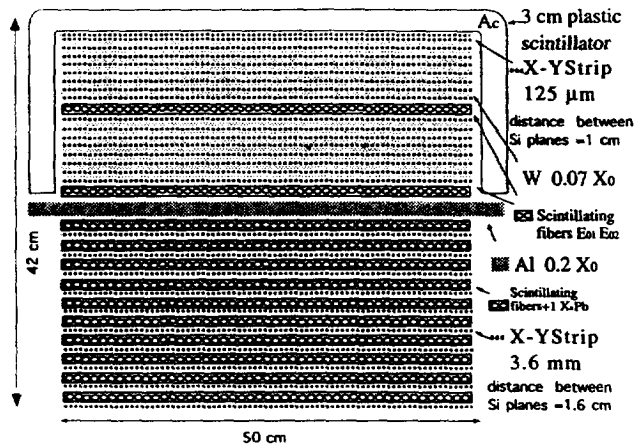


Figure 2. The stratigraphy of the GILDA B detector.

absence of pulses in the anticoincidence system:

$$C_1 \cdot C_2 \cdot C_3 \cdot \bar{A}_c$$

Thresholds of C_1 and C_2 have been chosen in order to provide a highly efficient registration of downward moving electromagnetic particles and eliminate upward moving ones. The second level trigger (slow) works after the readout and consists of an onboard analysis of the data from all the silicon strips; it requires, for a good gamma event, a spatial distribution of the energy deposition compatible with an electromagnetic shower. It will be possible to change, with telecommands from earth, the trigger configuration and the parameters that determine the energy thresholds, the aperture of the telescope and the counting rate.

2.2. Configuration B

We present also a version of GILDA where a new tracker, with higher spatial resolution and much larger read out channels, is adopted. This second and more sophisticated configuration of GILDA has a height of 42 cm, an area of 50×50 cm² and a total showering length of $11 X_0$, one in the tracker and 10 in the absorber.

A sketch of GILDA B is shown in figure

2. The first twenty planes form the converter zone, in which the silicon layers, made now of 125 μm strips, are separated by tungsten plates of thickness 0.07 X_0 . The distance between two contiguous planes is 1 cm. In each plane, 4000 silicon strips per view allow a very precise measurement of the direction of the gamma ray.

Like configuration A, an aluminum plate is placed between the converter and the absorber. The last ten planes, constituting the absorber, are composed of 3.6 mm silicon strips and separated by layers of active scintillating lead fibers, 1 X_0 total thickness. Silicon planes are 1.6 cm apart.

The structure of the scintillating fibers has been conceived embedding polystyrene scintillating fibers (1 mm of diameter) between plastic deformations of lead foils 0.5 mm thick. Prototypes have already been extensively tested [6,7] with accelerator beams, showing that the lead scintillating fibers calorimeter has a γ energy resolution of the order of $5\%/\sqrt{E(\text{GeV})}$ for total containment.

The configuration is completed with a plastic anticoincidence scintillator A_c (3 cm thick) around the converter zone, and with two fiber scintillators (without lead), one, E_{01} , after the first seven planes (after 0.49 X_0) and the other, E_{02} , after fourteen planes from the top of the detector. The introduction of the first one allows to obtain a lower threshold for γ detection of 25 MeV.

In this configuration, two triggers are adopted, for the low and high energy regions respectively:

- $\bar{A}_c \cdot (E_{01} \cdot OR \cdot E_{02})$, up to 1 GeV.
- for high energy, to avoid the same problems of EGRET, we do not use the anticoincidence scintillators. The trigger is constituted by the OR between E_{01} e E_{02} , with the request of having at least *two* of the following conditions for the energy deposited in the first planes of the absorber:

$$E_2 > E_1, \quad E_3 > E_2, \quad E_4 > E_3, \quad E_5 > E_4.$$

This imposes a shower behavior for an entering particle. In this case, the elimination of particles inducing hadronic showers is realized on board with the aid of pattern recognition algorithms.

	EGRET	GILDA B
Eff. area	0.16 m ²	0.14 m ² (0.5 GeV)
(area × efficiency)	0.12 m ²	0.13 m ² (1 GeV)
	0.07 m ²	0.17 m ² (10 GeV)
Point source	$6 \cdot 10^{-8}$	$6 \cdot 10^{-8}$ (0.1 GeV)
Sensitivity	$1 \cdot 10^{-8}$	$9 \cdot 10^{-10}$ (1 GeV)
(ph cm ⁻² s ⁻¹)	$1 \cdot 10^{-9}$	$1 \cdot 10^{-10}$ (10 GeV)
Volume	4.8 m ³	0.102 m ³
Mass	1830 kg	400 kg
Power	190 W	250 W

Table 1: *Some of the principal characteristics of GILDA B telescope compared with those of EGRET.*

3. Results

In figure 3 a comparison between GILDA A, GILDA B and EGRET energy resolutions is presented.

The total energy resolution of GILDA B calorimeter is $\sim 6\% / \sqrt{E(\text{GeV})}$ as far as the longitudinal leakage of the shower is negligible (≤ 1 GeV). The point marked as CsI is the energetic resolution of the calorimeter in case the lead scintillating fibers were substituted by CsI scintillators, option under study.

The results of our two telescopes angular resolution are plotted in figure 4 together with the EGRET ones.

Finally, in table 1 we report some geometrical characteristics of the GILDA B calorimeter, compared with EGRET ones (taken from [8]). Flux sensitivity is calculated at 5 σ detection threshold, 1 year data taking for GILDA and two week single point exposure for Egret. We assumed a background of $2 \cdot 10^{-5} \cdot (100 \text{ MeV}/E)^{1.1}$ ph⁻¹ cm⁻² s⁻¹ sr⁻¹, typical of the background seen by EGRET at high latitudes.

4. Conclusions

Our simulations have shown that the GILDA B instrument is able to reach significantly better performances than the experiment EGRET on the CGRO, though having less area and weight, for the following reasons:

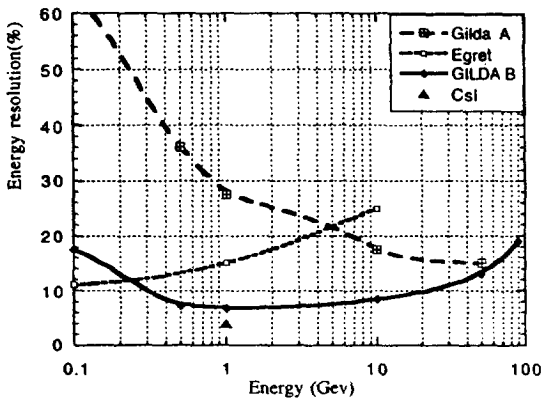


Figure 3. Simulated GILDA A and B energy resolution, compared with EGRET.

- the use of silicon strips instead of spark chambers as main device for reconstructing the gamma trajectory;
- the elimination of the anticoincidence counters for the high energy trigger, so that an efficiency of 70% up to 100 GeV can be reached;
- the elimination of TOF, with the consequent increase of the acceptance and decrease of the energetic detection threshold (25 MeV for GILDA and 35 for EGRET); again, the pattern recognition algorithms will substitute, off line, the TOF system, recognizing an upward going particle from a downward;
- the obtained compactness of the design which implies a very wide solid angle and so the possibility of monitoring many sources at the same time.

An important point is the modularity of our calorimeter that allows to easily change its lateral dimensions to tune the area, in an advanced project phase, to the maximum value permitted by the total weight of the payload. Of course, the collected statistics increases widening the area.

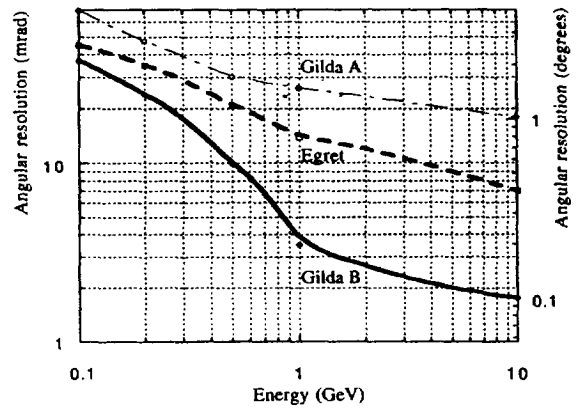


Figure 4. Simulated GILDA A and B angular resolution, compared with EGRET.

REFERENCES

1. Kanback G. et al., *Space Science Rev.*, **49**, 69, (1988).
Fichtel C. et al., *ApJ Supplement*, **94**, 551, (1994).
2. Golden, R. L. et al., *Il Nuovo Cimento*, **105 B**, 2, 191, (1990).
Barbiellini G. et al., *Il Nuovo Cimento*, **102 B**, 661, (1988).
3. Meschini M. et al., *Il Nuovo Cimento*, **102 B**, 523, (1988).
4. Bocciolini M. et al., *Nucl. Phys. B*, **32**, 77, (1993).
5. Bocciolini M. et al., *NIM*, **A333**, 560, (1993).
6. Hertzog D. W. et al., *NIM*, **A294**, 446, (1990).
7. Bianco S. et al., *NIM*, **A315**, 322, (1992).
8. Thompson D.J. et al., *ApJ Supplement*, **86**, 629, (1993).